

Small-Molecule Ligands as Potential GDNF Family Receptor Agonists

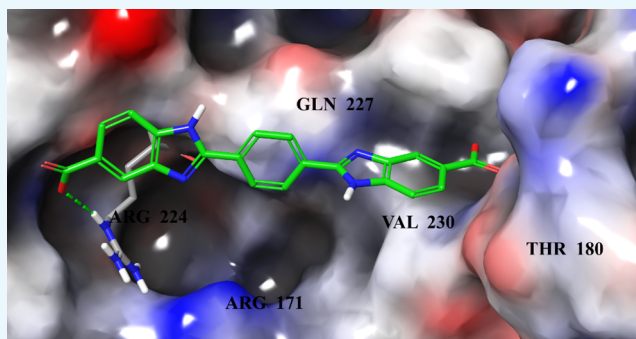
Larisa Ivanova,[†] Jaana Tammiku-Taul,[†] Yulia Sidorova,[‡] Mart Saarma,[‡] and Mati Karelson^{*†}

[†]Institute of Chemistry, University of Tartu, Ravila 14A, 50411 Tartu, Estonia

[‡]Laboratory of Molecular Neuroscience, Institute of Biotechnology, HiLIFE, University of Helsinki, Viikinkaari 5D, 00014 Helsinki, Finland

Supporting Information

ABSTRACT: To find out potential GDNF family receptor $\alpha 1$ (GFR $\alpha 1$) agonists, small molecules were built up by molecular fragments according to the structure-based drug design approach. Molecular docking was used to identify their binding modes to the biological target GFR $\alpha 1$ in GDNF-binding pocket. Thereafter, commercially available compounds based on the best predicted structures were searched from ZINC and MolPort databases (similarity $\geq 80\%$). Five compounds from the ZINC library were tested in phosphorylation and luciferase assays to study their ability to activate GFR $\alpha 1$ –RET. A bidental compound with two carboxyl groups showed the highest activity in molecular modeling and biological studies. However, the relative position of these groups was important. The meta-substituted structure otherwise identical to the most active compound 2-[4-(5-carboxy-1*H*-1,3-benzodiazol-2-yl)phenyl]-1*H*-1,3-benzodiazole-5-carboxylic acid was inactive. A weaker activity was detected for a compound with a single carboxyl group, that is, 4-(1,3-benzoxazol-2-yl)benzoic acid. The substitution of the carboxyl group by the amino or acetamido group also led to the loss of the activity.



INTRODUCTION

Glial cell line-derived neurotrophic factor (GDNF) family ligands (GFLs) consist of GDNF, neurturin (NRTN), artemin (ARTN), and persephin (PSPN).¹ GDNF and NRTN have demonstrated the ability to support the survival of brain dopamine-producing neurons, thus being potential therapeutic agents for Parkinson's disease.^{2–4} The survival of sympathetic and sensory neurons is supported by ARTN, and hence it has been considered for the treatment of chronic pain.⁵ However, the development of therapies for neurological diseases based on GFLs has serious problems associated with the delivery, stability, and potential side and off-target effects of these ligands.⁶ Therefore, the discovery of small molecules that bind to and activate GFL receptors would have large potential for the development of new strategies against neurodegenerative disorders.^{6–8} GDNF specifically binds to GDNF family receptor $\alpha 1$ (GFR $\alpha 1$), and then the complex binds to and signals through the transmembrane receptor tyrosine kinase RET. ARTN binds to GFR $\alpha 3$, NRTN to GFR $\alpha 2$, and also signal to the cells via RET.¹ Presently, structures of two scaffolds acting as the GDNF receptor agonists have been reported, XIB4035⁹ and BT13¹⁰ (Figure 1). Also BT13 derivative, compound called BT18 activates RET.¹¹

The aim of the current work was to find out new low molecular weight compounds acting as GFR $\alpha 1$ receptor agonists using the structure-based drug-design approach and molecular docking. The potential binding site for such agonists was searched by examining the protein–protein interactions on

the binding interface between GDNF and GFR $\alpha 1$ in the GDNF–GFR $\alpha 1$ –RET complex. A strong binding of a small-molecule ligand in this site could lead to the conformational changes and to the RET signaling.

RESULTS AND DISCUSSION

GDNF–GFR $\alpha 1$ Interface. Essential interactions at the binding interface between the GDNF and GFR $\alpha 1$ (i.e., hydrogen bonds and hydrophobic areas) were examined using the available crystal structures of the complex (PDB codes: 4UX8¹² and 3FUB;¹³ see Target in Methods). GFR $\alpha 1$ was treated as a receptor and GDNF as a ligand. There are several notable regions of the ligand–receptor interaction. First, three hydrogen bonds are formed by amine group of Arg171 and Arg224 (GFR $\alpha 1$) with oxygens of carboxylate group of Glu61 (GDNF). Three hydrogen bonds are also formed involving amine groups and carbonyl oxygens of peptide bond between Asn162 (GFR $\alpha 1$) and Glu62 (GDNF), Asn162 (GFR $\alpha 1$) and Ser112 (GDNF), and Arg224 (GFR $\alpha 1$) and Leu114 (GDNF). The hydroxyl groups of Ser172 (GFR $\alpha 1$) and Tyr120 (GDNF) are also hydrogen bond donors to the carbonyl oxygens of peptide bonds of Asp110 and Gln227, respectively (Figure 2). In addition, potential van der Waals

Received: December 5, 2017

Accepted: January 9, 2018

Published: January 25, 2018

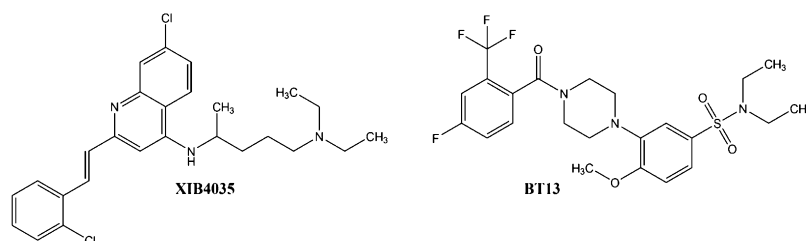


Figure 1. Chemical structures of XIB4035 and BT13.

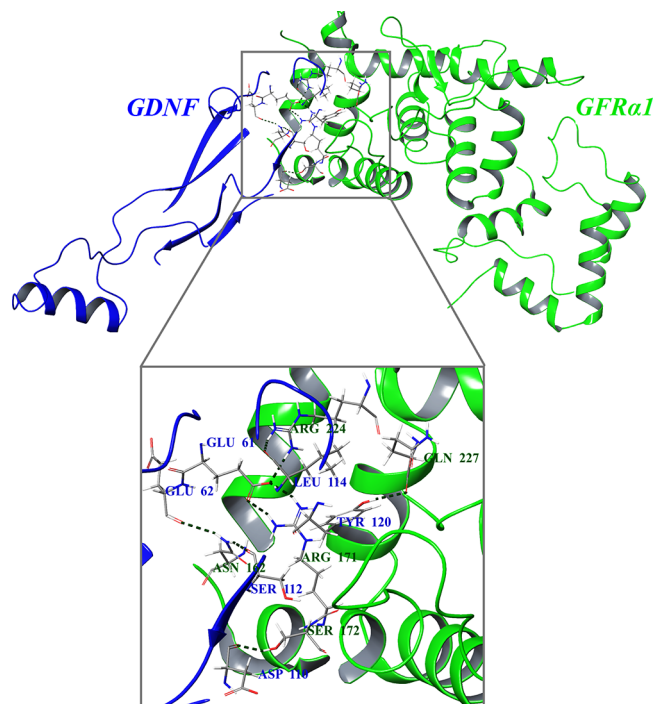


Figure 2. Analysis of interactions between GFR α 1 and GDNF residues (PDB code: 4UX8). The amino acid residues in the interface of GFR α 1 (green) and GDNF (blue) are colored as gray (carbon), blue (nitrogen), red (oxygen), and white (hydrogen). Hydrogen bonds are represented in green dashed lines.

interactions between the side groups of neighboring residues of the ligand, and the receptor can stabilize the binding complex (see Table S1 and Figure S1 in the [Supporting Information](#)). GDNF docking results are well in line with the previously published GFR α ^{14,15} and GDNF¹⁶ mutagenesis studies. Our assumption was that low-molecular-weight ligands (MW < 500) have to bind to residues of amino acids of GFR α 1, therefore imitating the native ligand GDNF. According to the analysis of binding site for the GFR α 1–GDNF complex, the key residues for interactions with a small molecule are Arg171 and Arg224 residues of the receptor which is in line with the previously published data.^{14,15} Consequently, the ligand acting as a potential receptor agonist has to be bound in the region of Thr179, Arg171, Arg224, and Gln227, forming hydrogen bonds to Arg171, Arg224, and/or Gln227.

Ligands Construction and Docking. The ligands were built up using molecular fragments that have significant docking binding to these receptor areas [see structure-based drug design (SBDD) approach in [Methods](#)]. The first group of ligand structures consisted of fragments of benzoate anion and its alkyl-substituted (Me, Et, and *i*-Pr) derivatives at the meta position. The length of the carbon chain (CH₂)_{*n*} of the

carboxylate substituent was also varied, with *n* = 0, 1, and 2 ([Figure 3A](#)). Thereafter, the heterocyclic derivatives were generated by the substitution of carbon atoms by up to two nitrogen atoms in the benzene ring ([Figure 3B](#)). The calculated binding energies for the studied 28 molecules from the first group of structures ([Table S2](#)) were in the range of -4.3 to -5.6 kcal/mol. Only one of the heterocyclic compounds (**25**) was able to demonstrate substantial specific binding, as illustrated in [Figure 4A](#), where the nitrogen atom of this compound is hydrogen bonded to the amine group of Arg171 and has additional van der Waals interactions with residues of Ile175, Thr179, Met211, Gln227, and Thr228. All results from the molecular docking calculations, that is, the corresponding binding energies and binding modes, are given in [Table S2](#) of the [Supporting Information](#).

The second group of the constructed GFR α 1 receptor ligands included 46 structures, where (i) at the R₂ position, hydrophobic alkyl group in the cyclic structures was substituted by hydroxyl, hydroxymethyl, amino, or aminomethyl groups ([Figure 3C](#)) enabling to form an additional hydrogen bond; (ii) more flexible cyclohexene ([Figure 3D](#)) or cyclohexanone basic structures ([Figure 3E](#)) were also used instead of rigid aromatic rings; and (iii) the carboxylate group was replaced by sulfonate group ([Figure 3F](#)), which can be strongly bound to proteins. The free energy of binding for all compounds was similar, which is in the range of -4.4 to -5.2 kcal/mol. Compounds consisting of more flexible cyclohexene or cyclohexanone rings as well as the sulfonate group did not have significantly lower binding energy. Most of the ligands of this subclass formed hydrogen bonds with the receptor by the carboxyl oxygens and/or by the added polar substituent at the R₂ position, by the nitrogen atom of the aromatic cycle, and by an oxygen atom of the sulfonate group ([Table S2](#)). As an example, compound **42** has two hydrogen bonds between its carboxyl oxygens and NH₂ group of Gln227 as well as between its CH₂OH group and NH group of Arg171 in addition to the interactions with Ile175, Met211, Arg224, and Thr228 ([Figure 4B](#)).

The third group of developed GFR α 1 receptor ligands was built using the following fragments: (i) flexible 5-oxocyclohex-3-ene-1-carboxylate, (ii) hydroxyl group, and (iii) hydroxyalkyl group (*n* of alkyl chain (CH₂)_{*n*} = 0–4; [Figure 3G](#)) or (2-hydroxyalkylcyclopropyl)methyl group (*n* of alkyl chain (CH₂)_{*n*} = 0–2; [Figure 3H](#)). The binding energies for these eight compounds ranged from -5.0 to -6.1 kcal/mol ([Table S2](#)). [Figure 4C](#) demonstrates the binding mode of compound **77**, which forms three hydrogen bonds by its carboxyl oxygens with amine group of Arg224, by hydroxypropyl group with the amine group of Gln227, and by hydroxyl group with carbonyl oxygen of Thr228 as well as van der Waals interactions with nearby residues of Arg171, Ile175, Met211, and Val230 of GFR α 1.

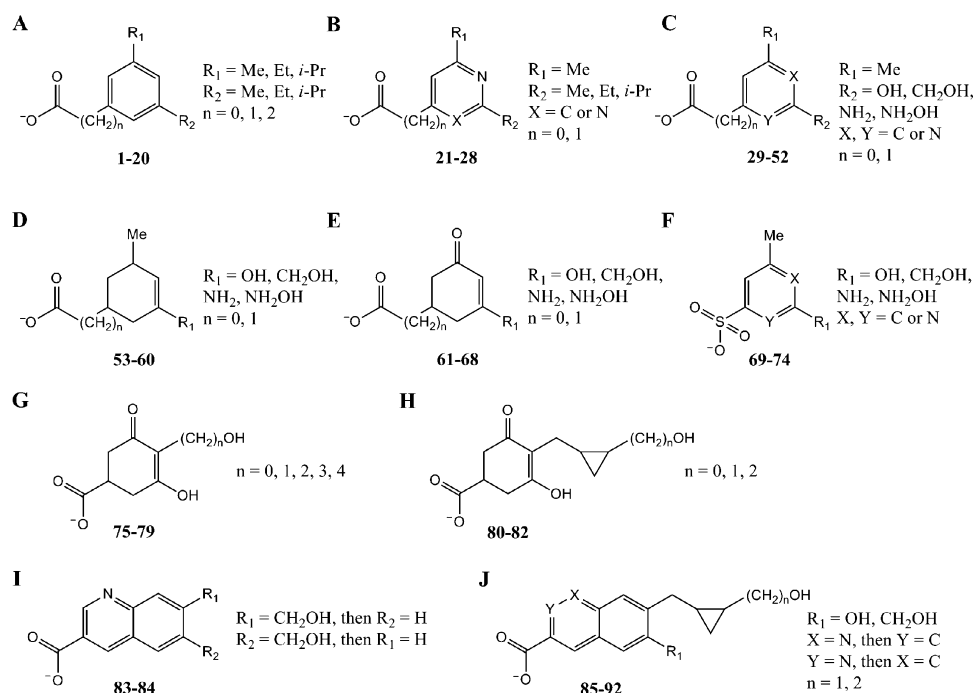


Figure 3. Structures of low-molecular-weight ligands used in the molecular docking to receptor $\text{GFR}\alpha_1$.

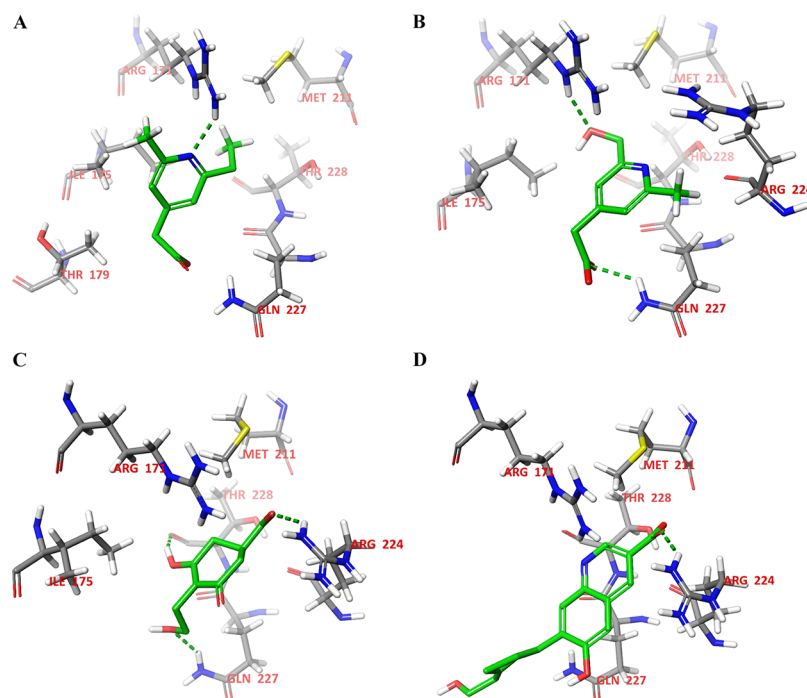


Figure 4. Calculated binding modes of compound **25** (A), compound **42** (B), compound **77** (C), and compound **86** (D) in the active site of $\text{GFR}\alpha_1$ (PDB code: 4UX8). The amino acid residues of $\text{GFR}\alpha_1$ are colored as gray (carbon), blue (nitrogen), red (oxygen), and white (hydrogen). Hydrogen bonds formed between compound and residues of $\text{GFR}\alpha_1$ are represented in green dashed lines.

According to the docking results on compounds from all these groups, we can conclude that (1) compounds with rigid aromatic ring(s) give somewhat lower binding energies than compounds with flexible cycles; (2) besides carboxyl functional group, hydroxyl group and its analogues as well as nitrogen atom of the heteroaromatic cycle may lead to additional hydrogen bonds with amino acid residues of $\text{GFR}\alpha_1$. Proceeding from these observations, the fourth group of 10 structures was constructed from fragments based on quinoline-

3-carboxylate or isoquinoline-3-carboxylate, hydroxyl or hydroxymethyl group, and (2-hydroxyalkylcyclopropyl)methyl group (Figure 3I,J). This group showed the lowest binding energies: -5.5 to -6.4 kcal/mol (Table S2). Surprisingly, only one hydrogen bond was formed through carboxyl oxygens of ligand to the amine group of Arg224 as demonstrated in Figure 4D for compound **86**, which has also van der Waals contacts with Arg171, Thr179, Met211, Gln227, and Thr228.

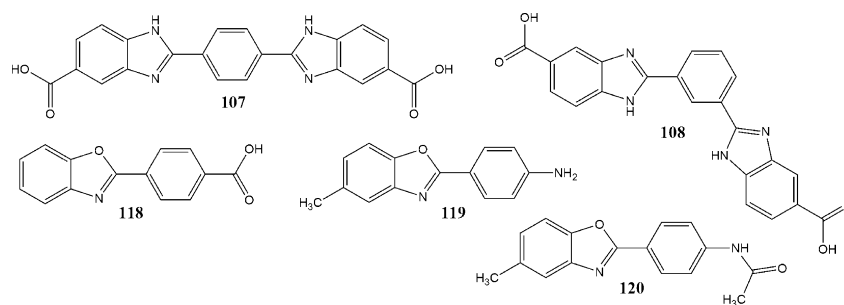


Figure 5. Compounds tested in luciferase assay in cells expressing GFR α 1–RET.

Testing of Potential GFR α 1 Receptor Agonists. On the basis of the last group of structures, similar compounds were searched from ZINC¹⁷ and MolPort¹⁸ databases (see Table S2). Five available compounds from the ZINC library (Figure 5) were initially tested in 5 and 20 μ M concentrations in luciferase assay in cells expressing GFR α 1–RET.¹⁹ Those ones activating luciferase by 1.5 times and above (compounds 107 and 118) were selected for dose-dependent experiments and RET phosphorylation (RET pY) assays (see Experimental Section); the remaining compounds were considered inactive (fold induction below 1.5 at 20 μ M) and excluded from further experiments. As predicted by the modeling, the bidental compound 107 with two carboxyl groups has the highest activity. Notably, a weak activity was detected for a much smaller compound 118 with a single carboxyl group in its structure. However, the relative position of these groups is important. The meta-substituted structure 108 otherwise identical to compound 107 is inactive. The substitution of the carboxyl group in compound 118 by the amino or acetamido group (compounds 119 and 120, respectively) also leads to the loss of the activity.

Thus, compounds 107 and 118 were tested in luciferase assay in six concentrations (0.1, 1, 5, 10, 25, and 50 μ M). Notably, compound 118 is a close derivative of the compound XIX described in the patent.²⁰ Application of 107 to GFR α 1–RET expressing cells led to moderate activation of luciferase [one-way analysis of variance (ANOVA) $F(12,39) = 33.11$] in 25 μ M (1526 ± 77.61 vs 514.8 ± 43.77 in control, $P < 0.0001$, one-way ANOVA with Dunnett's post hoc test) and 50 μ M concentrations (1963 ± 193.1 vs 514.8 ± 43.77 in control, $P < 0.0001$, one-way ANOVA with Dunnett's post hoc test), application of 50 μ M 118—to borderline activation of luciferase (956.3 ± 78.89 vs 514.8 ± 43.77 , $P = 0.0063$, one-way ANOVA with Dunnett's post hoc test) (Figure 6). To confirm luciferase assay results and evaluate the ability of these compounds to stimulate RET by direct methods, the selected compounds were tested in RET pY assays using western blotting. RET was immunoprecipitated, and western blotting membranes were probed first with antibodies against phosphorylated tyrosine residues (pY) and afterward—against RET protein to evaluate protein loading. Resulting images were quantified using Visual Studio software. Compound 118 failed to activate RET pY (relative intensity 0.70 ± 0.17 in control vs 0.64 ± 0.11 in compound-treated cell lysates, $N = 3$). Compound 107 activated RET pY in the cells expressing GFR α 1–RET but not in the cells expressing only RET (Figure 7A–C). Repeated measurements (RMs) ANOVA showed statistically significant differences between treatment groups in RET pY assay in both GFR α 1–RET ($P = 0.0020$, $F(1,120,5,601) = 28.31$) and GFP–RET ($P = 0.0219$,

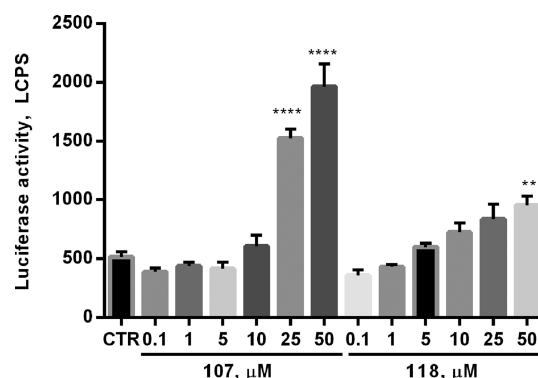


Figure 6. Dose-dependent activation of luciferase reporter gene in the cells expressing GFR α 1–RET receptor complex by compounds 107 and 118. Compounds are analyzed in quadruplicates. The results are presented as mean \pm SEM. **** $P < 0.0001$, ** $P < 0.01$, one-way ANOVA with the Dunnett's post hoc test. CTR—control.

$F(1,069,4,275)$) expressing cells (Figure 7B,C). Post hoc Dunnett's test revealed that compound 107 increased RET pY by 45% (relative intensity 0.68 ± 0.17 in control vs 0.99 ± 0.26 in compound-treated group, $P = 0.0405$, RM ANOVA with Dunnett's post hoc test) in GFR α 1–RET, but not in GFP–RET expressing cells (relative intensity 0.42 ± 0.16 in control vs 0.34 ± 0.077 in compound-treated group, $P = 0.693$ RM ANOVA with Dunnett's post hoc test). As expected, the positive controls (GDNF in GFR α 1–RET and soluble GFR α 1–GDNF complex in GFP–RET expressing cells) increased RET pY by 3.8-fold ($P = 0.0042$, RM ANOVA with Dunnett's post hoc test) and 4.9-fold ($P = 0.0465$, RM ANOVA with Dunnett's post hoc test) in GFR α 1–RET and GFP–RET expressing cells, respectively. These results indicate that compound 107 might, similarly to GDNF protein, require the presence of GFR α 1 coreceptor to stimulate RET pY.

The discrepancy between luciferase assay and RET pY assay data for compound 118 can be explained by the differences in the sensitivity of these assays. Luciferase assay is extremely sensitive and accumulates signals for the prolonged period of time that can include multiple cycles of RET and downstream signaling cascade activation, whereas RET pY assay is less sensitive and reflects activation of the receptor that is achieved at the moment of cell lysis. Another possibility is RET independent activation of luciferase in response to compound 118. Luciferase assay is designed to represent an activation of mitogen-activated protein kinase (MAPK) signaling pathway.¹⁹ This pathway includes multiple regulatory proteins that can be targeted by compound 118.

All corresponding binding modes obtained by molecular docking are illustrated in Figure 8. The most active compound

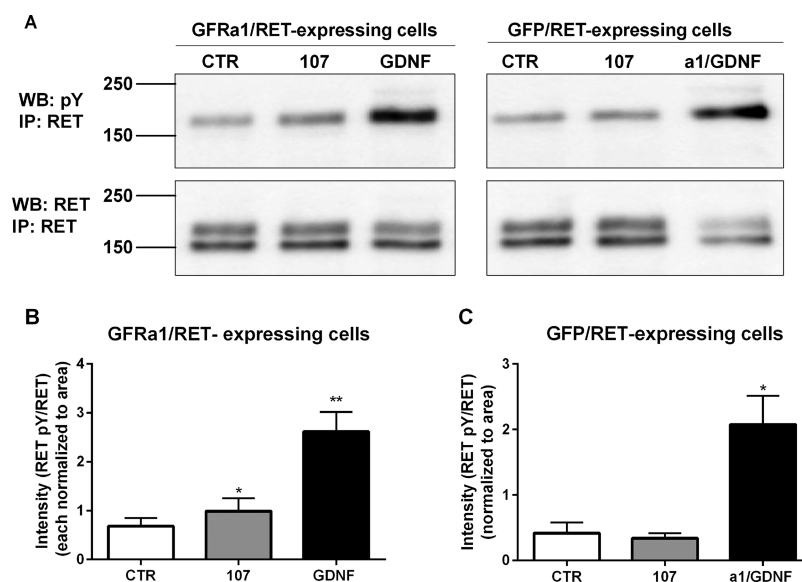


Figure 7. RET pY by compound **107** (100 μM) in MG87RET fibroblasts transiently transfected with GFR α 1 (B) and GFP (C). (A) Image of western blotting analysis. Molecular weight markers (in kDa) are indicated on the left. (B,C) Quantification of western blotting data. Quantitative data are presented as mean \pm SEM from 6 (B) or 5 (C) independent experiments. * $P < 0.05$, ** $P < 0.01$, RM ANOVA with the Dunnett's post hoc test. As a positive control, we used GDNF (100 ng/mL) in cell transfected with GFR α 1 (B) and soluble GFR α 1 (1 mg/mL) and GDNF (100 ng/mL) (a1/GDNF) in GFP-transfected cells (C). WB—western blotting, IP—immunoprecipitation.

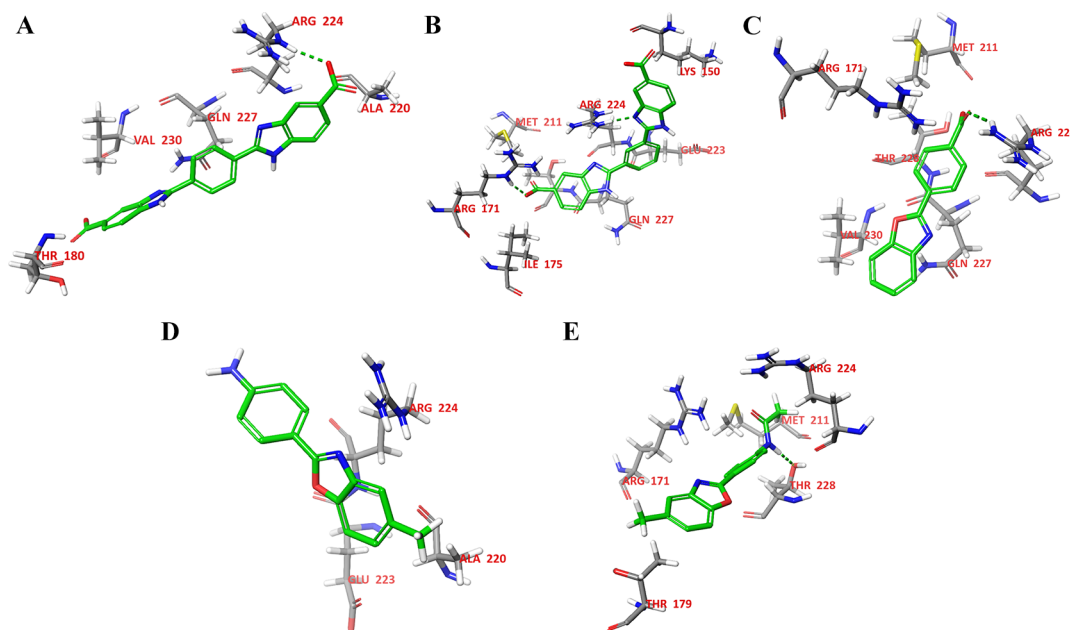


Figure 8. Calculated binding modes of compound **107** (A), compound **108** (B), compound **118** (C), compound **119** (D), and compound **120** (E) in the active site of GFR α 1 (PDB code: 4UX8). The amino acid residues of GFR α 1 are colored as gray (carbon), blue (nitrogen), red (oxygen), and white (hydrogen). Hydrogen bonds formed between compound and residues of GFR α 1 are represented in green dashed lines.

107 forms hydrogen bond by its carboxyl oxygens with NH group of Arg224 and interacts with Thr180, Ala220, Gln227, and Val230 (Figure 8A). The another potential GFR α 1 receptor agonist **118** has also one hydrogen bond between its carboxyl oxygens and amine group of Arg224 as well as van der Waals interactions with residues of Arg171, Met211, Gln227, Thr228, and Val230 (Figure 8C). Although inactive compounds **108** and **120** also form hydrogen bonds (Figure 8B,E), their molecular configuration can be different in solution and there is no binding. For instance, dipole moments μ are

different for para- and meta-substituted structures **107** and **108** ($\mu_{\text{para}} < \mu_{\text{meta}}$), respectively.

MD Simulations of GFR α 1–Ligand Complexes. To specify the nature of the ligand–protein interactions, the molecular mechanics/Poisson–Boltzmann surface area (MM/PBSA)²¹ binding energy calculations were carried out using data from molecular dynamics simulations. In MM/PBSA, the free energy of a state (ligand or protein) is estimated from the following sum

$$G = E_{\text{bnd}} + E_{\text{el}} + E_{\text{vdW}} + G_{\text{pol}} + G_{\text{np}} - TS \quad (1)$$

where the first three terms are standard molecular mechanics energy terms from bonded (bond, angle, and dihedral), electrostatic, and van der Waals interactions. G_{pol} and G_{np} are the polar and nonpolar contributions to the solvation free energies, respectively. G_{pol} is typically obtained by solving the Poisson–Boltzmann equation or by using the generalized Born model (giving the MM/GBSA approach), whereas the nonpolar term is estimated from a linear relation to the solvent accessible surface area. The last term in the above equation is the absolute temperature, T , multiplied by the entropy, S , estimated by a normal-mode analysis of the vibrational frequencies. The results for the lowest binding energy states for the complexes of compounds **107**, **108**, and **118** with GFR α 1 at the GDNF–GFR α 1 interface are given in Table 1.

Table 1. Binding Free Energies of the GFR α 1–Ligand Complexes Calculated Using the MM/PBSA Method^a

energy term	107 GDNF–GFR α 1 interface	108 GDNF–GFR α 1 interface	118 GDNF–GFR α 1 interface
ΔE_{vdw}	−37.01	−23.49	−23.04
ΔE_{el}	−137.78	−145.68	−96.96
ΔE_{pol}	137.94	151.83	97.82
ΔE_{np}	−19.37	−10.77	−16.79
ΔE_{bond}	−4.98	−5.29	−5.35
ΔG_{bind}	−53.38	−34.35	−44.02

^aAll energies in kcal/mol.

The binding free energy for the active para-substituted compound **107** is by 19.0 kcal/mol and by 9.4 kcal/mol lower than that for the inactive meta-substituted compound **108** and for compound **118** with weaker activity, respectively.

The binding mode of compound **107** was also confirmed by the counterpart molecular dynamics modeling. The simulations carried out at the GFR α 1 interface to GDNF indicated strong hydrogen bonding of the carboxylate groups of the ligand to the receptor residues Arg224 and Thr180 (Figures 9 and S2). This binding is complemented by the water-assisted binding of the

nitrogen atoms of the benzimidazole rings to residues Glu223 and Glu227.

It should be noted that this compound is very different from the earlier reported active compounds, that is, XIB4035⁹ and BT13.¹⁰ XIB4035 is unable to activate RET in the absence of endogenous ligand, that is, GFL,²² and BT13 is the RET agonist that is able to signal in the absence and presence of GFR α coreceptors. Therefore, compound **107** seems to represent a new scaffold that can be further optimized to develop efficient GFR α 1 agonists. Although weak biological activity of **107** makes the evaluation of its interaction with GFR α 1 difficult, biological data indicate that it might be the first compound activating GDNF receptor system via GFR α 1 coreceptor in the absence of endogenous GFL. Thus, further biochemical and cellular testing of such compounds have large biomedical interest.

METHODS

Structure-Based Drug Design. When the three-dimensional structure of biomolecular target is known, the SBDD approach can be applied in the drug discovery and development process.^{23,24} The task is to design small molecules (receptor agonists) that will fit to the binding pocket of the target (hydrophobic surfaces, hydrogen bonding sites, etc.), and the binding affinity will be predicted by a fast approximate docking program. Ligands are built up by molecular fragments using “linkers” or “scaffolds”, if necessary, within the constraints of the binding site in the case of de novo method. The compounds constructed this way have to correspond to Lipinski’s rule of five.²⁵

Target. We proceeded from two available crystal structures on the GDNF–GFR α 1 complex downloaded from Protein Data Bank. The hybrid structural model of reconstituted mammalian GDNF–GFR α 1–RET complex (i.e., RET ternary complex; code: 4UX8) had been derived from electron microscopy and low-angle X-ray scattering data with a resolution of 24.0 Å.¹² The protein consists of chain A and chain B (RET; residues 29–508), chain C and chain E (GFR α 1; residues 6–348), and chain D and chain F (GDNF; residues 42–134). The crystal structure of the GDNF–GFR α 1 tetrameric

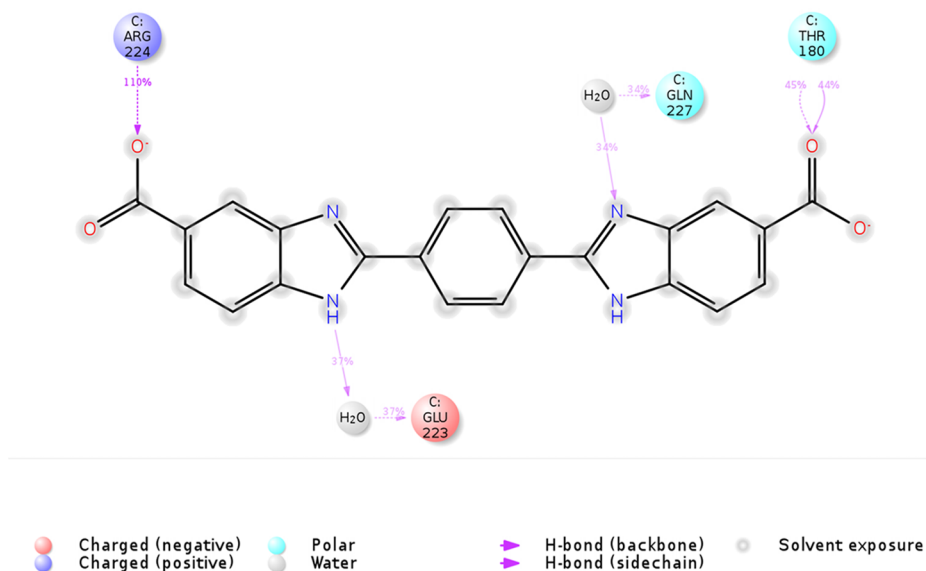


Figure 9. Calculated binding mode of compound **107** by the molecular dynamics simulations.

complex (code: 3FUB) was measured by X-ray diffraction with a resolution of 2.35 Å.¹³ The asymmetric unit contains two chains of GFR α 1 (chain A, residues 150-348; chain C, residues 150-348) and two chains of GDNF (chain B, residues 40-134; chain D, residues 32-134).

Both raw crystal structures were corrected, and hydrogen atoms were automatically added to the protein using Schrödinger's Protein Preparation Wizard of Maestro 10.7.²⁶ AutoDockTools (ADT)²⁷ 1.5.6 was used to identify the binding interface between the chains of GDNF and GFR α 1. As hydrogen bonds and van der Waals interactions were largely identical in both crystal structures, thus, chains C and D of GDNF–GFR α 1–RET complex (code: 4UX8) was used for the further study. Water molecules were removed from the crystal structure.

Small-Molecule Library. The initial data set for virtual fragment-based docking screening was constructed by molecular fragments in a way that compounds would be bound to the biological target GFR α 1 similarly to GDNF. Commercially available compounds based on these structures and using Tanimoto similarity coefficient ($\geq 80\%$) were searched from ZINC¹⁷ and MolPort¹⁸ databases. The two-dimensional chemical structures of ligands were converted into three-dimensional structures and preoptimized by molecular mechanics MM+ field using HyperChem 8.0.²⁸ The "Online SMILES Translator and Structure File Generator"²⁹ program was used to create pdb files for molecular docking procedure.

Molecular Docking. AutoDock Vina 1.1.2³⁰ was used for the docking studies to find out binding modes and binding energies of ligands to the receptor. The number of rotatable bonds of ligand was set by default by ADT.²⁷ However, if the number was greater than 6, then some of rotatable bonds was made as nonrotatable, otherwise calculations can be inaccurate.³¹ The active binding site on GFR α 1, obtained by the removal of GDNF (chain D), was surrounded with a grid box sized 30 \times 30 \times 30 points with a spacing of 1.000 Å. The settings used for the iterated local search global optimizer based on mutation and local optimization steps, accepted or rejected with a Metropolis criterion in Vina, were nine modes, one central processing unit, and an energy range of 1 kcal/mol. Other settings were used as default.

Molecular Dynamics. The molecular dynamics simulations were carried out using Desmond simulation package of Schrödinger LLC.³² The NPT ensemble with the temperature of 300 K and a pressure of 1 bar was applied in all runs. The simulation lengths were 10 and 50 ns with a relaxation time of 1 ps. The OPLS_2005 force field parameters were used in all simulations.³³ The long-range electrostatic interactions were calculated using the particle mesh Ewald method.³⁴ The cutoff radius in Coulomb' interactions was 9.0 Å. The water molecules were described using simple point charge model.³⁵ The Martyna–Tuckerman–Klein chain coupling scheme³⁶ with a coupling constant of 2.0 ps was used for the pressure control and the Nosé–Hoover chain coupling scheme³⁶ for the temperature control. Nonbonded forces were calculated using an r-RESPA integrator where the short-range forces were updated every step and the long-range forces were updated every three steps. The trajectories were saved at 4.8 ps intervals for analysis. The behavior and interactions between the ligands and protein were analyzed using the Simulation Interaction Diagram tool implemented in Desmond molecular dynamics package. The stability of molecular dynamics simulations was

monitored by looking on the root mean square deviation of the ligand and protein atom positions in time.

Experimental Section. Compounds. Experimentally studied compounds were purchased from MolPort Inc.¹⁸

Proteins. GDNF was obtained from Icosagen Ltd. (Cat# P-103-100).

Plasmids. Full-length human GFR α 1 cDNA¹⁹ subcloned in pCDNA6 (Invitrogen), full-length human RET (long isoform) in pCR3.1 (Invitrogen),³⁷ enhanced GFP-expressing vector—pEGFP-N1 (Clontech, Cat# 6085-1, discontinued), and PathDetect Elk-1 system (Stratagene) to detect MAPK activation.

Cell Lines. MG87RET murine fibroblasts stably transfected with RET proto-oncogene.¹⁶ Reporter gene systems to detect MAPK activation: MG87RET stably transfected with PathDetect Elk-1 and GFR α 1 or empty vector.¹⁹

Luciferase Assays. To identify compounds activating GFLs receptors and check their ability to activate intracellular signaling via RET, we used previously developed reporter-gene-based system (MG87 murine fibroblast stably transfected with PathDetect Elk-1, GFR α 1, and RET).¹⁹ The day before the experiment, the reporter cells were plated into 96-well plates (PerkinElmer) at 175 000 to 200 000 cell/mL density in Dulbecco's Modified Eagle's medium (DMEM), 10% fetal bovine serum, 100 μ g/mL Normocin (InvivoGen, Cat# ant-nr-1), 1% dimethyl sulfoxide (DMSO), and 15 mM Hepes pH 7.2. The next day compounds or proteins under study were applied to the cells in desirable concentrations. The following day, the cells were lysed and luciferase activity was measured using the neolite luciferase detection reagent (PerkinElmer, Cat# 6016711). The luminescence was measured using a plate luminometer (Optima FW, Thermo Scientific). At first compounds were tested in triplicates in two concentrations (5 and 20 μ M). Compounds activating luciferase in initial screen by 1.5-fold or above at least in one concentration were further subjected to the analysis in 6 concentrations (0.1, 1, 5, 10, 25, and 50 μ M). Dose-dependent studies were made in quadruplicates.

RET Phosphorylation Assay. MG87RET cells were plated on 35 mm tissue culture dishes 2 days before the experiment to achieve 90–95% of confluency of the cells at the day of stimulation with tested substances. The next day, cells were transfected with 4 μ g/well of GFR α 1- or GFP-expressing plasmid using Lipofectamine 2000 (Invitrogen) for DNA delivery as described by the manufacturer. On the third day, cells were starved in serum-free DMEM containing 15 mM Hepes, pH 7.2, and 1% DMSO for 4 h and stimulated with compounds or GDNF. Then, cells were washed once with ice-cold phosphate-buffered saline containing 1 mM Na₃VO₄ and 1 mM NaF and lysed on ice in 0.5 mL per well of RIPA-modified buffer (50 mM Tris-HCl, pH 7.4, 150 mM NaCl, 1 mM ethylenediaminetetraacetic acid (EDTA), 1% NP-40, 1% TX-100, 10% glycerol, EDTA-free protease inhibitor cocktail (Roche), 1 mM Na₃VO₄, 2.5 mg/mL of sodium deoxycholate, 1 mM NaF). Plates were incubated at +4 °C on the horizontal shaker for 30 min with vigorous shaking; lysates were collected to the Eppendorf tubes and centrifuged for 10 min at +4 °C at 13 000 rpm to precipitate cell debris.

To immunoprecipitate RET cell lysates were incubated overnight at +4 °C on the round rotator in the presence of 1 μ g/mL of goat anti-RET C-20 antibodies (Santa Cruz Biotechnology Cat# sc-1290, RRID:AB_631316) and magnetic beads conjugated with protein G (Dynabeads, Thermo Fisher

Scientific, Cat# 10004D). Beads were washed three times with 1× tris-buffered saline (TBS) with 1% triton X-100; bound proteins were eluted by 100 μL of 2× Laemmli loading buffer, resolved on 7.5% sodium dodecyl sulfate polyacrylamide gel and then transferred onto a nitrocellulose membrane. Membrane was blocked for 15 min at room temperature with TBS-T (1× TBS containing 0.15% Tween 20) containing 10% skimmed milk and probed with antiphosphotyrosine antibodies (Millipore, Cat# 05-321, RRID:AB_309678) diluted 1:1500 in TBS-T with 3% skimmed milk for 2 h at room temperature. The membranes were washed three times for 5 min in TBS-T and incubated in the 1:1000 solution of secondary antimouse antibodies conjugated with HRP (DAKO, Cat# P0447) diluted in TBS-T containing 3% skimmed milk for 45 min at room temperature. Membranes were washed with TBS-T for 4 × 10 min. Stained bands were visualized with a Pierce ECL western blotting substrate (Cat# 32106) or SuperSignal ELISA Femto substrate (Pierce, Cat# 37075) using LAS-3000 imaging software. To confirm, equal loading membranes were stripped and re-probed with anti-RET C-20 antibodies (1:500) diluted in TBS-T containing 3% skimmed milk. To detect C-20, we used secondary antigoat antibodies conjugated with HRP (1:1500, DAKO, Cat# P0449).

Quantification of RET Phosphorylation. Quantification of RET pY images was done using Image Studio 5.2 software. Intensities of the bands corresponding to phosphorylated surface form of RET (MW = 170 kDa) and total surface form of RET were first normalized to their areas and intensity/area values for RET pY band then were normalized to the intensity/area values of RET band. The images from 3 to 6 independent experiments were quantified.

Statistical Analysis. Quantitative data were analyzed by one-way or RM ANOVA with the Dunnett's post hoc test to determine the significance of the differences. *P* values below 0.05 were considered statistically significant.

■ ASSOCIATED CONTENT

● Supporting Information

The Supporting Information is available free of charge on the ACS Publications website at DOI: 10.1021/acsomega.7b01932.

Analysis of the GDNF–GFR α 1 interface; molecular docking results for small-molecule ligands to the receptor GFR α 1; molecular dynamics calculated contacts between compound 107 and GFR α 1 (PDF)

■ AUTHOR INFORMATION

Corresponding Author

*E-mail: mati.karelson@ut.ee (M.K.).

Author Contributions

L.I. performed molecular docking and molecular dynamics simulations; L.I., J.T.-T., and M.K. analyzed modeling results. Y.S. performed biological experiments; Y.S. and M.S. analyzed experimental data. M.K. coordinated the project. All authors participated in the preparation of the manuscript and approved the final manuscript.

Notes

The authors declare no competing financial interest.

■ ACKNOWLEDGMENTS

Current work was financially supported by (i) the EU European Regional Development Fund through the Center of Excellence in Molecular Cell Engineering (project no. 2014-2020.4.01.15-

0013), Estonia; (ii) Estonian Research Council (PUT-582); (iii) FP7-HEALTH-2013-INNOVATION-1 GA N602919. We thank Jenni Montonen, Elena Burtovskaia, Jaime Calvo Sanches, and Piotr Michalowski for their excellent assistance with experimental procedures.

■ REFERENCES

- (1) Airaksinen, M. S.; Saarma, M. The GDNF family: signalling, biological functions and therapeutic value. *Nat. Rev. Neurosci.* **2002**, *3*, 383–394.
- (2) Domanskyi, A.; Saarma, M.; Airavaara, M. Prospects of Neurotrophic Factors for Parkinson's Disease: Comparison of Protein and Gene Therapy. *Hum. Gene Ther.* **2015**, *26*, 550–559.
- (3) Ibáñez, C. F.; Andressoo, J.-O. Biology of GDNF and its receptors\Relevance for disorders of the central nervous system. *Neurobiol. Dis.* **2017**, *97*, 80–89.
- (4) Marks, W. J.; Ostrem, J. L.; Verhagen, L.; Starr, P. A.; Larson, P. S.; Bakay, R. A.; Taylor, R.; Cahn-Weiner, D. A.; Stoessl, A. J.; Olanow, C. W.; Bartus, R. T. Safety and tolerability of intraputamin delivery of CERE-120 (adeno-associated virus serotype 2–neurturin) to patients with idiopathic Parkinson's disease: an open-label, phase I trial. *Lancet Neurol.* **2008**, *7*, 400–408.
- (5) Gardell, L. R.; Wang, R.; Ehrenfels, C.; Ossipov, M. H.; Rossomando, A. J.; Miller, S.; Buckley, C.; Cai, A. K.; Tse, A.; Foley, S. F.; Gong, B.; Walus, L.; Carmillo, P.; Worley, D.; Huang, C.; Engber, T.; Pepinsky, B.; Cate, R. L.; Vanderah, T. W.; Lai, J.; Sah, D. W. Y.; Porreca, F. Multiple actions of systemic artemin in experimental neuropathy. *Nat. Med.* **2003**, *9*, 1383–1389.
- (6) Sidorova, Y. A.; Saarma, M. Glial cell line-derived neurotrophic factor family ligands and their therapeutic potential. *Mol. Biol.* **2016**, *50*, 521–531.
- (7) Beshpalov, M. M.; Saarma, M. GDNF family receptor complexes are emerging drug targets. *Trends Pharmacol. Sci.* **2007**, *28*, 68–74.
- (8) Sidorova, Y. A.; Beshpalov, M. M.; Karelson, M.; Saarma, M. Small Molecular Weight ARTN Mimetic for the Treatment of Neuropathic Pain. *Cell Transplant.* **2012**, *21*, 792.
- (9) Tokugawa, K.; Yamamoto, K.; Nishiguchi, M.; Sekine, T.; Sakai, M.; Ueki, T.; Chaki, S.; Okuyama, S. XIB4035, a novel nonpeptidyl small molecule agonist for GFR α -1. *Neurochem. Int.* **2003**, *42*, 81–86.
- (10) Sidorova, Y. A.; Beshpalov, M. M.; Wong, A. W.; Kambur, O.; Jokinen, V.; Lilius, T. O.; Suleymanova, I.; Karelson, G.; Rauhala, P. V.; Karelson, M.; Osborne, P. B.; Keast, J. R.; Kalso, E. A.; Saarma, M. A Novel Small Molecule GDNF Receptor RET Agonist, BT13, Promotes Neurite Growth from Sensory Neurons in Vitro and Attenuates Experimental Neuropathy in the Rat. *Front. Pharmacol.* **2017**, *8*, No. 365.
- (11) Beshpalov, M. M.; Sidorova, Y. A.; Suleymanova, I.; Thompson, J.; Kambur, O.; Jokinen, V.; Lilius, T.; Karelson, G.; Puusepp, L.; Rauhala, P.; Kalso, E.; Karelson, M.; Saarma, M. Novel agonist of GDNF family ligand receptor RET for the treatment of experimental neuropathy. **2016**, BioRxiv 10.1101/061820.
- (12) Goodman, K. M.; Kjær, S.; Beuron, F.; Knowles, P. P.; Nawrotek, A.; Burns, E. M.; Purkiss, A. G.; George, R.; Santoro, M.; Morris, E. P.; McDonald, N. Q. RET Recognition of GDNF-GFR α 1 Ligand by a Composite Binding Site Promotes Membrane-Proximal Self-Association. *Cell Rep.* **2014**, *8*, 1894–1904.
- (13) Parkash, V.; Goldman, A. Comparison of GFL–GFR α complexes: further evidence relating GFL bend angle to RET signalling. *Acta Crystallogr., Sect. F: Struct. Biol. Cryst. Commun.* **2009**, *65*, 551–558.
- (14) Leppänen, V.-M.; Beshpalov, M. M.; Runeberg-Roos, P.; Puurand, Ü.; Merits, A.; Saarma, M.; Goldman, A. The structure of GFR α 1 domain 3 reveals new insights into GDNF binding and RET activation. *EMBO J.* **2004**, *23*, 1452–1462.
- (15) Parkash, V.; Leppänen, V.-M.; Virtanen, H.; Jurvansuu, J. M.; Beshpalov, M. M.; Sidorova, Y. A.; Runeberg-Roos, P.; Saarma, M.; Goldman, A. The structure of the glial cell line-derived neurotrophic

factor-coreceptor complex: insights into RET signaling and heparin binding. *J. Biol. Chem.* **2008**, *283*, 35164–35172.

(16) Eketjäll, S.; Fainzilber, M.; Murray-Rust, J.; Ibáñez, C. F. Distinct structural elements in GDNF mediate binding to GFR α 1 and activation of the GFR α 1-c-Ret receptor complex. *EMBO J.* **1999**, *18*, 5901–5910.

(17) Irwin, J. J.; Sterling, T.; Mysinger, M. M.; Bolstad, E. S.; Coleman, R. G. ZINC: a free tool to discover chemistry for biology. *J. Chem. Inf. Model.* **2012**, *52*, 1757–1768.

(18) <http://www.molport.com/shop/index>; MolPort: Lacplesa iela 41, Riga, LV-1011, Latvia.

(19) Sidorova, Y. A.; Mätlik, K.; Paveliev, M.; Lindahl, M.; Piranen, E.; Milbrandt, J.; Arumäe, U.; Saarma, M.; Bespalov, M. M. Persephin signaling through GFR α 1: The potential for the treatment of Parkinson's disease. *Mol. Cell. Neurosci.* **2010**, *44*, 223–232.

(20) Saarma, M.; Karelson, M.; Bespalov, M.; Pilv, M. Methods of facilitating neural cell survival using GDNF family ligands (GFL) mimetics or RET signaling pathway activators. U.S. Patent 8,901,129 B2, 2014.

(21) Genheden, S.; Ryde, U. The MM/PBSA and MM/GBSA methods to estimate ligand-binding affinities. *Expert Opin. Drug Discovery* **2015**, *10*, 449–461.

(22) Hedstrom, K. L.; Murtie, J. C.; Albers, K.; Calcutt, N. A.; Corfas, G. Treating small fiber neuropathy by topical application of a small molecule modulator of ligand-induced GFR α /RET receptor signaling. *Proc. Natl. Acad. Sci. U.S.A.* **2014**, *111*, 2325–2330.

(23) Anderson, A. C. The Process of Structure-Based Drug Design. *Chem. Biol.* **2003**, *10*, 787–797.

(24) Aparoy, P.; Reddy, K. K.; Reddanna, P. Structure and Ligand Based Drug Design Strategies in the Development of Novel 5-LOX Inhibitors. *Curr. Med. Chem.* **2012**, *19*, 3763–3778.

(25) (a) Lipinski, C. A.; Lombardo, F.; Dominy, B. W.; Feeney, P. J. Experimental and computational approaches to estimate solubility and permeability in drug discovery and development settings. *Adv. Drug Delivery Rev.* **2001**, *46*, 3–26. (b) Lipinski, C. A. Lead- and drug-like compounds: the rule-of-five revolution. *Drug Discovery Today: Technol.* **2004**, *1*, 337–341.

(26) (a) Sastry, G. M.; Adzhigirey, M.; Day, T.; Annabhimoju, R.; Sherman, W. Protein and ligand preparation: Parameters, protocols, and influence on virtual screening enrichments. *J. Comput.-Aided Mol. Des.* **2013**, *27*, 221–234. *Schrödinger Release 2016-3: Schrödinger Suite 2016-3 Protein Preparation Wizard*; Epik, Schrödinger, LLC: New York, NY, 2016; Impact, Schrödinger, LLC, New York, NY, 2016; Prime, Schrödinger, LLC, New York, NY, 2016.

(27) Morris, G. M.; Huey, R.; Lindstrom, W.; Sanner, M. F.; Belew, R. K.; Goodsell, D. S.; Olson, A. J. Autodock4 and AutoDockTools4: automated docking with selective receptor flexibility. *J. Comput. Chem.* **2009**, *16*, 2785–2791.

(28) *HyperChem 8.0 Molecular Modeling Package*; Hypercube Software: Gainesville, FL.

(29) <https://cactus.nci.nih.gov/translate/>.

(30) Trott, O.; Olson, A. J. AutoDock Vina: improving the speed and accuracy of docking with a new scoring function, efficient optimization, and multithreading. *J. Comput. Chem.* **2010**, *31*, 455–461.

(31) Höltje, H.-D.; Folkers, G. Small Molecules. In *Molecular Modeling: Basic Principles and Applications*; Mannhold, R., Kubinyi, H., Timmerman, H., Eds.; Wiley-VCH Verlag GmbH: Weinheim, Germany, 1996; pp 9–63.

(32) *Schrödinger Release 2017-3: Desmond Molecular Dynamics System*; D. E. Shaw Research: New York, NY, 2017.

(33) Banks, J. L.; Beard, H. S.; Cao, Y.; Cho, A. E.; Damm, W.; Farid, R.; Felts, A. K.; Halgren, T. A.; Mainz, D. T.; Maple, J. R.; Murphy, R.; Philipp, D. M.; Repasky, M. P.; Zhang, L. Y.; Berne, B. J.; Friesner, R. A.; Gallicchio, E.; Levy, R. M. Integrated Modeling Program, Applied Chemical Theory (IMPACT). *J. Comput. Chem.* **2005**, *26*, 1752–1780.

(34) Toukmaji, A. Y.; Board, J. A., Jr. Ewald Summation Techniques in Perspective: A Survey. *Comput. Phys. Commun.* **1996**, *95*, 73–92.

(35) Zielkiewicz, J. Erratum: Structural Properties of Water: Comparison of the SPC, SPCE, TIP4P, and TIP5P Models of Water. *J. Chem. Phys.* **2006**, *124*, 109901.

(36) Martyna, G. J.; Klein, M. L.; Tuckerman, M. Nosé–Hoover Chains: The Canonical Ensemble via Continuous Dynamics. *J. Chem. Phys.* **1992**, *97*, 2635–2643.

(37) Runeberg-Roos, P.; Virtanen, H.; Saarma, M. RET(MEN 2B) is active in the endoplasmic reticulum before reaching the cell surface. *Oncogene* **2007**, *26*, 7909–7915.